

Evaluation of myocardial blood flow and coronary flow reserve after implantation of a bioresorbable vascular scaffold versus metal drug-eluting stent: an interim one-month analysis of the VANISH trial



Wijnand J. Stuijzand¹, MD; Pieter G. Raijmakers², MD, PhD; Roel S. Driessen¹, MD; Adriaan A. Lammertsma², PhD; Albert C. van Rossum¹, MD, PhD; Alexander Nap¹, MD, PhD; Yolande Appelman¹, MD, PhD; Jorrit S. Lemkes¹, MD; Maarten A. van Leeuwen¹, MD; Niels van Royen¹, MD, PhD; Paul Knaapen^{1*}, MD, PhD

1. Department of Cardiology, VU University Medical Center, Amsterdam, The Netherlands; 2. Radiology & Nuclear Medicine, VU University Medical Center, Amsterdam, The Netherlands

KEYWORDS

- bioresorbable vascular scaffold
- cold pressor test
- coronary flow reserve
- myocardial blood flow
- percutaneous coronary intervention
- positron emission tomography

Abstract

Aims: A randomised clinical trial of bioresorbable vascular scaffold (BVS) vs. metal drug-eluting stent (DES) was initiated, using positron emission tomography (PET) perfusion imaging to assess the effects of both treatments on (hyperaemic) myocardial blood flow (MBF) and coronary flow reserve (CFR) over a three-year period (VANISH trial). In the present study, early, i.e., after one month, MBF and CFR are reported.

Methods and results: Sixty patients (45 men [75%], 55±7 years) with a documented single-vessel type A or B1 lesion were included in this single-blind randomised clinical trial. Patients were randomised to implantation of a BVS or DES in a one-to-one fashion. Approximately one month after percutaneous coronary intervention, patients underwent [¹⁵O]H₂O PET to assess (hyperaemic) MBF, cold pressor test MBF, and CFR. One patient refused PET perfusion at one-month follow-up (in the DES arm). MBF of the treated myocardial territory during rest, CPT, and hyperaemia were not different in BVS-treated patients as compared to DES-treated patients (1.02±0.28 vs. 0.96±0.24 mL·min⁻¹·g⁻¹, p=0.38, 1.20±0.38 vs. 1.08±0.23 mL·min⁻¹·g⁻¹, p=0.16, and 3.04±0.80 vs. 3.33±0.77 mL·min⁻¹·g⁻¹, p=0.16, respectively). CFR of the treated myocardial territory was significantly lower in the BVS-treated patients (3.09±0.94 vs. 3.57±0.85, p<0.05).

Conclusions: No differences in PET-derived absolute myocardial perfusion were observed between BVS-treated patients as compared to DES-treated patients at one-month follow-up. CFR was attenuated in BVS-treated patients, although still within the normal range.

*Corresponding author: Department of Cardiology, VU University Medical Center, De Boelelaan 1117, 1081 HV Amsterdam, The Netherlands. E-mail: p.knaapen@vumc.nl

Abbreviations

BVS	bioresorbable vascular scaffold
CAD	coronary artery disease
CFR	coronary flow reserve
CPT	cold pressor test
DES	drug-eluting stent
ICA	invasive coronary angiography
MBF	myocardial blood flow
OCT	optical coherence tomography
PCI	percutaneous coronary intervention
PET	positron emission tomography
QCA	quantitative coronary angiography

Introduction

The bioresorbable vascular scaffold (BVS) has been developed as a novel approach for the percutaneous treatment of coronary artery disease (CAD). After implantation, a BVS provides six to 12 months support to the vessel wall before gradually dissolving in the following two-year period. Regression of the scaffold stimulates remodelling of the natural vessel wall as a result of renewed exposure to pulsatile flow, shear stress, and cyclic strain patterns, potentially circumventing some of the long-term hazards of permanent metal coronary drug-eluting stents (DES)¹⁻⁴. Released from the metal “cage”, the originally stented coronary segment may become responsive to physiological stimuli with revival of normal vasomotor functions^{5,6}. Furthermore, a recent interim report of the randomised ABSORB II trial described a reduction of cumulative rates of new or worsening angina from up to 30 days after treatment with BVS in comparison with metal stents⁷. Although additional research is warranted to clarify and substantiate this observation, it is hypothesised that restoration of normal coronary physiology and enhanced conformability of the BVS contribute to improved clinical outcome^{7,8}. Compared with DES, however, a relatively diminished acute lumen gain and increased midterm (six months) lumen loss have been documented after BVS implantation in the ABSORB trials^{7,9-12}. Therefore, a randomised clinical trial of BVS vs. metal DES was initiated, utilising positron emission tomography (PET) perfusion imaging to assess (hyperaemic) myocardial blood flow (MBF), MBF during a cold pressor test (CPT), and coronary flow reserve (CFR) over a three-year period (VANISH trial, NCT01876589)¹³. In the present report, results of the ongoing VANISH trial at one-month follow-up are presented, investigating whether lower cumulative rates of angina after BVS can be explained by enhanced MBF and CFR.

Methods

STUDY DESIGN AND PARTICIPANTS

The VANISH trial is a prospective, single-blind, randomised, two-group, single-centre clinical trial. Eligible participants were 18-66 years old with *de novo* flow-limiting single-vessel CAD (type A or B1 lesions) without biochemical signs of myocardial infarction and with a normal left ventricular function ($\geq 50\%$). Exclusion criteria were prior cardiac history, poor kidney function

(eGFR < 30 ml·min⁻¹), asthma, other than sinus rhythm, or pregnancy. Patients were randomised to implantation of a BVS or metal DES using Absorb or XIENCE PRIME® (Abbott Vascular, Santa Clara, CA, USA), in a one-to-one fashion. Patients were blinded as to the implanted study device. Study investigators and operators were instructed not to disclose treatment assignment to patients and referring physicians. Follow-up using [¹⁵O]H₂O PET to assess baseline MBF, CPT MBF, hyperaemic MBF, and CFR was planned approximately one month, one year, and three years after percutaneous coronary intervention (PCI). Furthermore, re-invasive coronary angiography (ICA) with optical coherence tomography (OCT) of the treated coronary segment will be performed at three-year follow-up. The primary study design aimed to include 60 participants in order to provide 90% power to detect a 10% difference in hyperaemic MBF, assuming completed study protocols in at least 50 subjects. The study was approved by the ethics committee of the VU University Center and written informed consent was obtained from all patients.

PERCUTANEOUS CORONARY INTERVENTION AND OPTICAL COHERENCE TOMOGRAPHY

ICA and PCI were performed on a biplane or monoplane cardiovascular X-ray system (Allura Xper FD 10/10; Philips Healthcare, Best, The Netherlands). Selection of device dimensions was guided by OCT or quantitative coronary angiography (QCA). Implantation of DES and BVS was performed according to standard procedural guidelines and choice of post-dilatation was left to the discretion of the operator. The study device had to cover at least 2 mm of non-diseased tissue on either side of the target lesion. Post-dilatation was allowed with a balloon shorter than the implanted device. When additional bailout stenting was required, an additional investigational device was implanted. Intravascular OCT was performed prior to and immediately after device implantation with automated injection of three or four ml·sec⁻¹ contrast agent. Automated pullback was set at 20 mm/sec⁻¹ and was manually initiated. OCT image quality was instantly interpreted and OCT was repeated according to the judgement of the operator until sufficient image quality was obtained. All patients will receive at least 80 mg of aspirin daily for the study duration and 75 mg of clopidogrel daily for a minimum of 12 months after PCI.

OPTICAL COHERENCE TOMOGRAPHY

Measurements were analysed by an analyst blinded to the PET perfusion results with patented offline software (ILUMIEN™ OPTIS™; LightLab Imaging/St. Jude Medical, St. Paul, MN, USA). Analyses of continuous cross-sections were performed at each longitudinal frame within the treated segment. Mean and minimal luminal areas, and mean and minimal luminal diameters were calculated using semi-automated endoluminal contour detection, and were manually adjusted if necessary¹². By using the endoluminal vessel wall contour, the device struts of both BVS and DES were included in the luminal dimensions in case of good apposition or malapposition.

However, delineation within the strut area was performed in case of vessel wall prolapse protruding through the device struts¹².

PET IMAGING

PET studies using oxygen-15 labelled water were performed as described previously¹⁴. Briefly, patients were scanned on an Ingenuity TF 128 PET/CT scanner (Philips Healthcare). All patients were asked to refrain from any caffeine or xanthine containing products for 24 hours prior to scanning. Vasoactive medication was ceased temporarily at least five pharmacological half-lives prior to the scan. After a scout CT for patient positioning, a dynamic emission scan was performed at rest followed by two identical scans during CPT and intravenous adenosine ($140 \mu\text{g}\cdot\text{kg}^{-1}\cdot\text{min}^{-1}$) induced hyperaemia (**Figure 1**). CPT was performed by immersing the right hand of the patient into melting ice water, starting at least 90 seconds prior to the start of the scan, and was continued for at least 7.5 minutes¹⁵. After 60 to 90 seconds, patients were asked to provide a level of pain according to a 10-point scale. Low-dose CT scans were used to correct for scatter and attenuation¹⁶. Parametric MBF images were generated and analysed quantitatively by an experienced analyst using Cardiac VUer¹⁷. The analyst was blinded for all other study results. MBF was expressed in $\text{mL}\cdot\text{min}^{-1}\cdot\text{g}^{-1}$ of perfusable tissue. MBF during rest, CPT, and hyperaemia was calculated for each of the following three vascular territories, left anterior descending (LAD), circumflex (Cx), and right coronary artery (RCA), according to standard segmentation procedures¹⁸. CFR was calculated as the ratio of hyperaemic MBF to baseline MBF whereas CPT reserve was calculated as the ratio of CPT MBF to baseline MBF for each of the vascular territories. To account for changes in CFR caused by cardiac workload at baseline, baseline MBF values were corrected for the rate pressure product. Corrected baseline MBF was calculated by multiplying 10,000 by the ratio of baseline MBF and rate pressure product. The corrected CFR was defined as the ratio of hyperaemic MBF and the corrected baseline MBF. Target area was defined as the myocardial territory of a treated vessel, whilst

remote myocardium was defined as the myocardial territory of the remaining non-treated vessels.

STATISTICAL ANALYSIS

Continuous variables are presented as mean values \pm standard deviation (SD), whereas categorical variables are expressed as actual numbers. Continuous variables of paired data were compared with the paired samples t-test, whereas comparisons between groups were performed using the two independent samples t-test, unless stated otherwise. Differences in proportions between groups were assessed with the Pearson chi-square or Fisher's exact test, depending on the expected frequency of categories. Statistical analyses were performed using SPSS software, Version 20.0 (IBM Corp., Armonk, NY, USA)

Results

From August 2013 to December 2014, 60 patients were enrolled successfully and randomised to implantation of BVS versus DES in a one-to-one ratio. Baseline characteristics are listed in **Table 1**. In both the BVS and DES arms, all devices were implanted successfully. BVS was implanted with lower driving pressure and post balloon dilatation was performed more often to achieve appropriate device apposition. Culprit lesions were predominantly located in the LAD ($n=36$, 60%) and less frequently in the RCA ($n=14$, 23%), or Cx ($n=10$, 17%). Bail-out stenting was required in three culprit lesions (all DES arm), either to seal a proximal ($n=1$) or distal ($n=1$) edge dissection or because of initial lesion length underestimation ($n=1$). The average device length was comparable between both treatment arms. Due to a small side branch occlusion, one patient (BVS arm) suffered from a periprocedural myocardial infarction without Q-wave occurrence and minimal cardiac enzyme release (CKMB max of 32.4 U/l^{-1}). Procedural characteristics are shown in **Table 2**. One patient from the DES arm declined PET perfusion at one-month follow-up and was excluded for PET perfusion analysis. Apart from the single aforementioned periprocedural myocardial

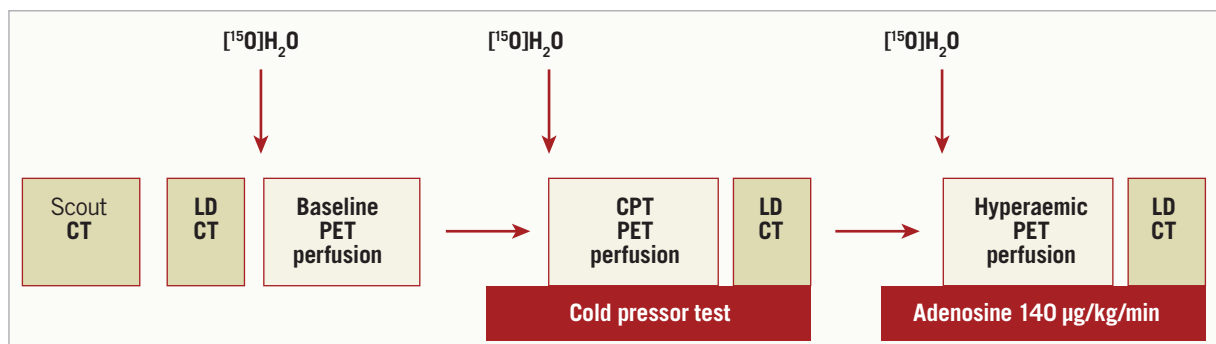


Figure 1. PET perfusion protocol. Schematic illustration of the PET protocol at one month after BVS and DES implantation. PET perfusion imaging was performed during resting conditions (baseline), followed by two identical PET sequences during CPT and intravenously administered adenosine (hyperaemia). BVS: bioresorbable vascular scaffold; CPT: cold pressor test; CT: computed tomography; DES: drug-eluting stent; LD: low-dose; $[^{15}\text{O}]\text{H}_2\text{O}$: oxygen labelled water; PET: positron emission tomography

Table 1. Baseline patient characteristics (n=60).

Characteristic		All N (%) or mean±SD	BVS N (%) or mean±SD	DES N (%) or mean±SD	p-value
BVS vs. DES	Age (years)	55±7	55±7	55±7	0.78
	Male	45 (75%)	23 (77%)	22 (73%)	0.77
	Body mass index (kg·m ⁻²)	27.2±4.7	26.7±4.9	27.7±4.5	0.43
CAD risk factors	Hypertension	30 (50%)	15 (50%)	15 (50%)	1.00
	Hypercholesterolaemia	16 (27%)	8 (27%)	8 (27%)	1.00
	Current smoking	29 (48%)	18 (60%)	11 (37%)	0.12
	History of smoking	12 (20%)	3 (10%)	9 (30%)	0.10
	Family history CAD	34 (57%)	17 (57%)	17 (57%)	1.00
	Diabetes	6 (10%)	2 (7%)	4 (13%)	0.67
Medication	Aspirin	57 (95%)	28 (93%)	29 (97%)	1.00
	ACE inhibitors	24 (40%)	12 (40%)	12 (40%)	1.00
	Beta-blockers	54 (90%)	27 (90%)	27 (90%)	1.00
	Statins	54 (90%)	27 (90%)	27 (90%)	1.00
	Dual antiplatelets	32 (53%)	16 (53%)	16 (53%)	1.00
	Long-acting nitrates	6 (10%)	2 (7%)	4 (13%)	0.67
Indication	Stable angina	42 (70%)	18 (60%)	24 (80%)	0.16
	Silent ischaemia	1 (2%)	–	1 (3%)	1.00
	Unstable angina	17 (28%)	12 (40%)	5 (17%)	0.08
Culprit arteries	LAD	36 (60%)	16 (53%)	20 (67%)	0.43
	RCA	14 (23%)	6 (20%)	8 (27%)	0.76
	CX	10 (17%)	8 (27%)	2 (7%)	0.08

ACE: angiotensin-converting enzyme; BVS: bioresorbable vascular scaffold; CAD: coronary artery disease; Cx: circumflex; DES: drug-eluting stent; LAD: left anterior descending; RCA: right coronary artery; SD: standard deviation

infarction, no major adverse cardiac events were registered during the first month of follow-up.

OPTICAL COHERENCE TOMOGRAPHY

Representative OCT images prior to and immediately after BVS and DES implantation are shown in **Figure 2**. In one patient OCT was not obtained due to the inability to provide an injection with sufficient contrast through a 5 Fr guiding catheter (the initial 6 Fr radial access procedure was converted to a 5 Fr guide due to radial artery spasm and patient discomfort). In four patients OCT image quality was considered insufficient to perform proper luminal analyses. This was mainly due to inadequate positioning of the guiding catheter resulting in insufficient contrast. In the remaining 55 patients OCT was performed successfully immediately after device implantation. Mean and minimal luminal areas, and mean and minimal

luminal diameters post device implantation were comparable between both treatment arms (**Table 3**).

HAEMODYNAMIC CONDITIONS DURING PET

Haemodynamic conditions during baseline, CPT, and hyperaemic PET scans are summarised in **Table 4**. Blood pressure increased significantly during CPT in comparison with baseline, whilst heart rate was significantly higher during hyperaemia PET. There were no differences in heart rate, blood pressure, or rate pressure product between treatment arms (all $p>0.05$).

BASELINE MYOCARDIAL BLOOD FLOW

PET perfusion measurements were performed successfully in 59 patients at 35±9 days post PCI. **Table 5** summarises quantitative perfusion values of global, target, and remote areas in both treatment arms. Global MBF at baseline was 0.99±0.27 mL·min⁻¹·g⁻¹

Table 2. Percutaneous coronary intervention characteristics.

	All (n=60)	BVS (n=30)	DES (n=30)	p-value
Post-dilatation, n (%)	33 (55%)	21 (70%)	12 (40%)	0.02
Implantation pressure (atm)	13.4±3.3	12.5±3.3	14.3±3.0	0.03
Maximal dilatation pressure (atm)	16.1±4.0	16.2±4.6	15.9±3.3	0.82
Maximal diameter (mm)	3.61±0.39	3.59±0.34	3.63±0.44	0.69
Unforeseen additional device implantation, n (%)	3 (5%)	0 (0%)	3 (10%)	na
Average device length (mm)	24.2±6.1	24.3±4.9	24.1±7.2	0.90

atm: atmosphere; BVS: bioresorbable vascular scaffold; DES: drug-eluting stent; mm: millimetres; na: not applicable

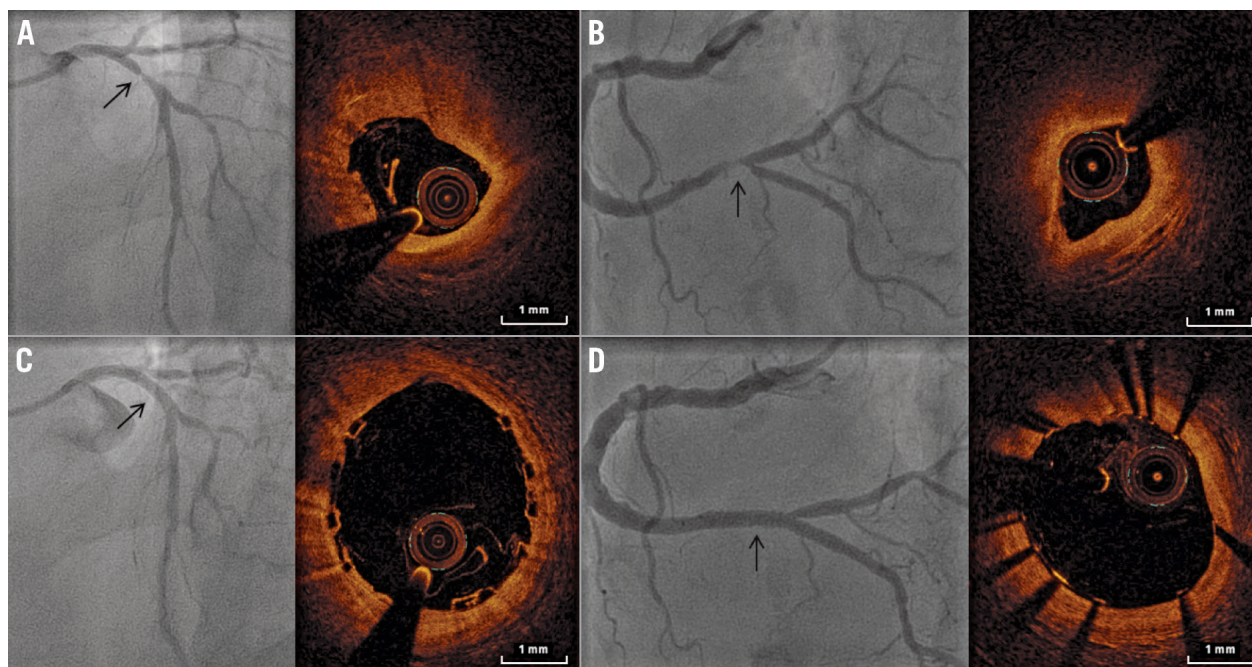


Figure 2. ICA and OCT of BVS and DES. Representative ICA and OCT images prior to and after BVS and DES implantation. A) A severely stenosed proximal LAD on ICA (arrow), and OCT of the most affected segment. This lesion was successfully treated with a BVS, as shown on ICA (arrow) and OCT immediately after implantation (B). C) ICA and OCT of a high-grade distal RCA stenosis (arrow), with a good angiographic and OCT result after DES implantation (D, arrow). BVS: bioresorbable vascular scaffold; DES: drug-eluting stent; ICA: invasive coronary angiography; LAD: left anterior descending coronary artery; OCT: optical coherence tomography; RCA: right coronary artery

(BVS vs. DES; 1.02 ± 0.29 vs. 0.96 ± 0.24 mL · min⁻¹ · g⁻¹, $p=0.37$). Target and remote baseline MBF were comparable between BVS and DES arms ($p \geq 0.05$ for both).

COLD PRESSOR TEST MYOCARDIAL BLOOD FLOW

The reported 10-point-scaled pain score during CPT was 6.2 ± 1.4 . Quantitative perfusion of the target area increased significantly from baseline to CPT ($p < 0.001$) (Table 5). There were no significant differences in CPT quantitative perfusion or CPT reserve between treatment arms of the target (BVS vs. DES; $p=0.16$ and $p=0.69$, respectively) (Figure 3) and remote area ($p=0.22$ and $p=0.38$, respectively).

HYPERAEMIC MYOCARDIAL BLOOD FLOW

Global MBF during hyperaemia was 3.12 ± 0.78 mL · min⁻¹ · g⁻¹ (BVS vs. DES; $p=0.22$) (Table 5). Target (Figure 4) and remote hyperaemic MBF were comparable between BVS and DES arms ($p=0.16$ and $p=0.25$, respectively).

CORONARY FLOW RESERVE

A typical example of PET CFR in a case of BVS and one of DES can be seen in Figure 5. A trend for a globally attenuated CFR was observed ($p=0.06$) in the BVS treatment arm, whilst CFR of the target area was significantly lower in the BVS arm than in the DES arm (3.09 ± 0.94 vs. 3.57 ± 0.85 , $p < 0.05$) (Table 5, Figure 4). In addition, a trend towards a lower CFR was observed in remote areas of the BVS arm ($p=0.06$). Target area CFR in relation to remote area CFR (CFR target/CFR remote) was comparable between both treatment arms ($p=0.62$) (Table 5). Correction for baseline rate pressure product (RPP) increased the significance levels of CFR differences between the BVS and DES arms for global, target, and remote areas (all $p < 0.01$) (Table 5).

Discussion

The present interim analysis of the VANISH trial was conducted to evaluate myocardial perfusion at one month after BVS and

Table 3. Optical coherence tomography parameters immediately after PCI.

	All (n=55)	BVS (n=27)	DES (n=28)	p-value (BVS vs. DES)
Mean luminal area (mm ²)	7.91 ± 1.88	7.71 ± 1.68	8.10 ± 2.06	0.45
Minimal luminal area (mm ²)	5.79 ± 1.76	5.64 ± 1.50	5.94 ± 2.00	0.55
Mean luminal diameter (mm)	3.14 ± 0.37	3.10 ± 0.35	3.18 ± 0.40	0.43
Minimal luminal diameter (mm)	2.69 ± 0.39	2.65 ± 0.35	2.73 ± 0.43	0.45

BVS: bioresorbable vascular scaffold; DES: drug-eluting stent; mm: millimetres; PCI: percutaneous coronary intervention

Table 4. Haemodynamic conditions during PET at baseline, CPT, and hyperaemia.

Parameter		All devices (n=59)	BVS (n=30)	DES (n=29)	p-value (BVS vs. DES)
Heart rate (bpm)	Baseline	65±11	66±11	65±12	0.94
	CPT	68±12	70±11	67±13	0.47
	Hyperaemia	88±17	86±18	90±16	0.37
	P-value baseline CPT	<0.01	<0.01	0.02	
	P-value baseline hyperaemia	<0.01	<0.01	<0.01	
Systolic blood pressure (mmHg)	Baseline	126±18	123±16	130±20	0.16
	CPT	142±25	141±27	143±24	0.76
	Hyperaemia	129±19	127±17	132±21	0.35
	P-value baseline CPT	<0.01	<0.01	<0.01	
	P-value baseline hyperaemia	0.13	0.13	0.51	
Diastolic blood pressure (mmHg)	Baseline	69±8	69±8	70±8	0.32
	CPT	76±11	77±11	76±10	0.60
	Hyperaemia	67±9	67±9	67±10	0.72
	P-value baseline CPT	<0.01	<0.01	<0.01	
	P-value baseline hyperaemia	0.04	0.10	0.24	
Mean arterial pressure (mmHg)	Baseline	88±10	87±10	90±11	0.36
	CPT	98±15	98±15	98±14	0.94
	Hyperaemia	88±11	87±10	89±12	0.46
	P-value baseline CPT	<0.01	<0.01	<0.01	
	P-value baseline hyperaemia	0.66	0.80	0.72	
Rate pressure product	Baseline	8,273±1,969	8,043±1,568	8,511±2,317	0.37
	CPT	9,738±2,573	9,805±2,448	9,669±2,737	0.84
	Hyperaemia	11,327±2,773	10,824±2,461	11,848±3,017	0.16
	P-value baseline CPT	<0.01	<0.01	<0.01	
	P-value baseline hyperaemia	<0.01	<0.01	<0.01	

bpm: beats per minute; BVS: bioresorbable vascular scaffold; CPT: cold pressor test; DES: drug-eluting stent; PET: positron emission tomography

Table 5. Myocardial perfusion.

		All (n=59)	BVS (n=30)	DES (n=29)	p-value (BVS vs. DES)
Global	MBF baseline (mL·min ⁻¹ ·g ⁻¹)	0.99±0.27	1.02±0.29	0.96±0.24	0.37
	CPT (mL·min ⁻¹ ·g ⁻¹)	1.11±0.29	1.16±0.34	1.06±0.23	0.20
	CPT reserve	1.13±0.16	1.14±0.16	1.12±0.16	0.60
	MBF hyperaemia (mL·min ⁻¹ ·g ⁻¹)	3.12±0.78	3.00±0.78	3.25±0.78	0.22
	CFR	3.26±0.90	3.04±0.86	3.49±0.90	0.06
	RPP corrected CFR	2.63±0.66	2.41±0.62	2.87±0.64	<0.01
Target area	MBF baseline (mL·min ⁻¹ ·g ⁻¹)	0.99±0.26	1.02±0.28	0.96±0.24	0.38
	CPT (mL·min ⁻¹ ·g ⁻¹)	1.14±0.32	1.20±0.38	1.08±0.23	0.16
	CPT reserve	1.16±0.23	1.18±0.20	1.15±0.26	0.69
	MBF hyperaemia (mL·min ⁻¹ ·g ⁻¹)	3.18±0.79	3.04±0.80	3.33±0.77	0.16
	CFR	3.32±0.92	3.09±0.94	3.57±0.85	<0.05
	RPP corrected CFR	2.68±0.69	2.44±0.67	2.93±0.63	<0.01
Remote area	MBF baseline (mL·min ⁻¹ ·g ⁻¹)	1.00±0.29	1.03±0.32	0.96±0.25	0.35
	CPT (mL·min ⁻¹ ·g ⁻¹)	1.11±0.30	1.15±0.34	1.06±0.24	0.22
	CPT reserve	1.13±0.17	1.14±0.18	1.12±0.17	0.38
	MBF hyperaemia (mL·min ⁻¹ ·g ⁻¹)	3.11±0.80	2.99±0.78	3.22±0.81	0.25
	CFR	3.25±0.93	3.03±0.86	3.48±0.96	0.06
	RPP corrected CFR	2.61±0.69	2.39±0.62	2.84±0.68	<0.01
CFR target vs. remote ratio		1.03±0.13	1.02±0.13	1.04±0.13	0.62

BVS: bioresorbable vascular scaffold; CFR: coronary flow reserve; CPT: cold pressor test; DES: drug-eluting stent; MBF: myocardial blood flow; RPP: rate pressure product

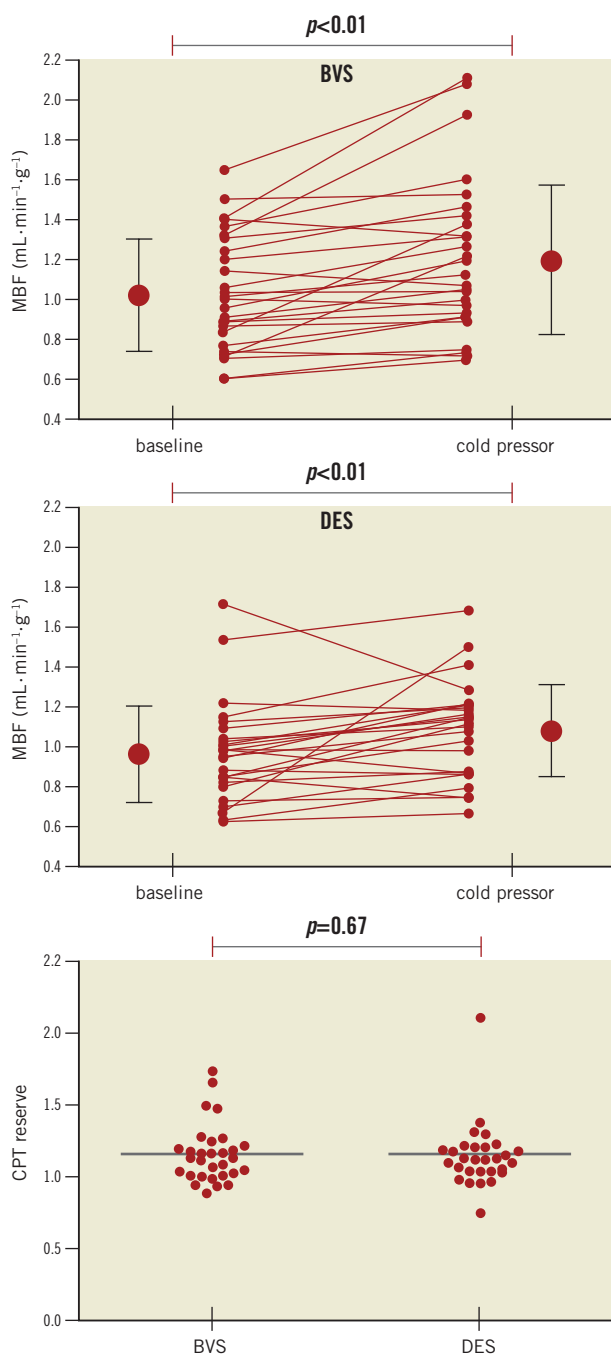


Figure 3. Myocardial blood flow response to cold pressor testing. MBF of the target area increased significantly ($p < 0.01$) from baseline to CPT in both the BVS and DES arms. No differences in CPT reserve were observed between both treatment groups. CPT: cold pressor test; BVS: bioresorbable vascular scaffold; DES: drug-eluting stent; MBF: myocardial blood flow

DES implantation. The results indicate that myocardial perfusion of the treated vascular territory and remote area at baseline, CPT, and hyperaemia are comparable between the BVS and DES arms. Only CFR was significantly lower in the target area after BVS implantation. In addition, a trend towards lower CFR was also observed in remote areas in BVS-treated patients. Nevertheless,

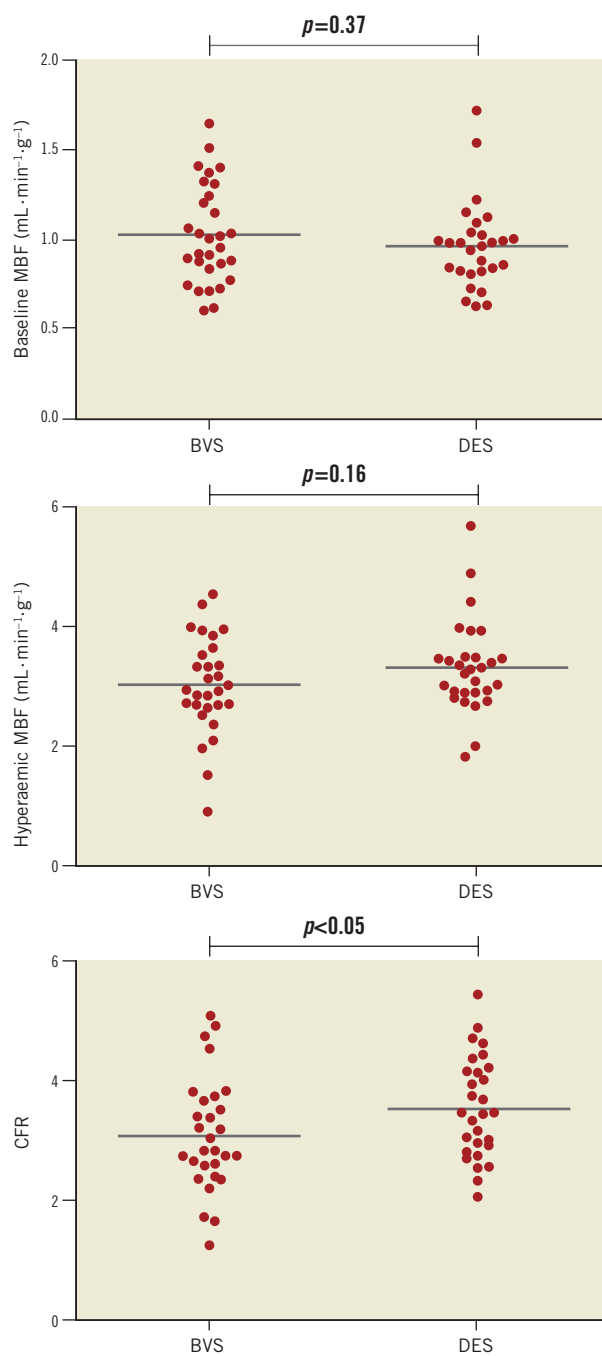


Figure 4. Baseline MBF, hyperaemic MBF, and CFR of both the BVS and DES treatment arms. Baseline and hyperaemic MBF were comparable between BVS and DES-treated vessels; however, CFR of the target area was significantly lower in the BVS arm. BVS: bioresorbable vascular scaffold; CFR: coronary flow reserve; DES: drug-eluting stent; MBF: myocardial blood flow

the ratio of target CFR to remote CFR was comparable between both treatment arms.

PROCEDURAL CHARACTERISTICS

The vulnerable BVS design mandates careful implantation instructions¹⁹. BVS was employed with lower driving pressure and

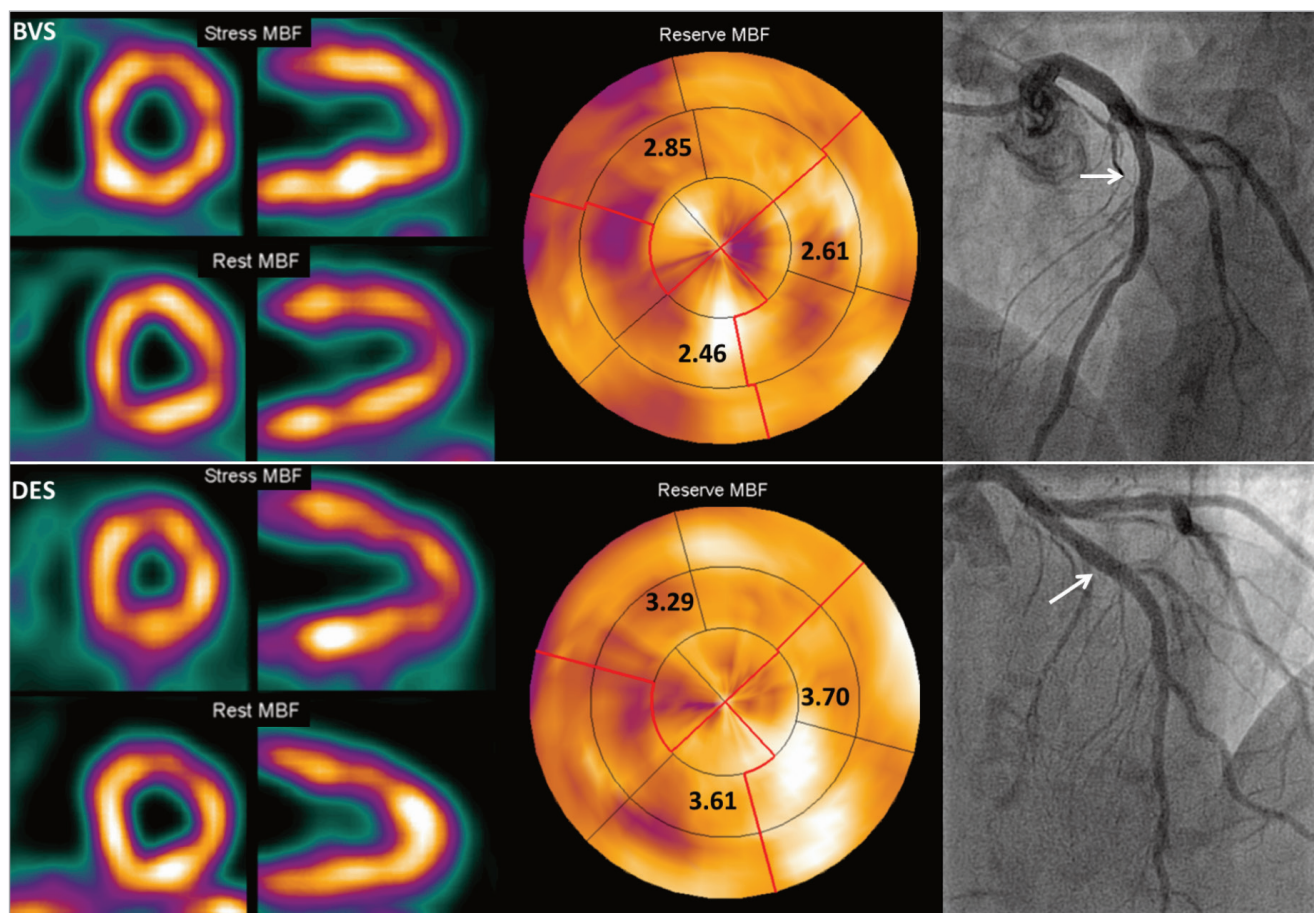


Figure 5. PET results of two patients after BVS or DES implantation. Completely normal baseline MBF, hyperaemic MBF, and CFR one month after implantation of BVS (upper row) and DES (lower row) of a proximal LAD with an excellent angiographic result (white arrows). Although both CFR results are well above clinical cut-off values (2.5), this example illustrates the attenuated CFR after BVS in comparison with DES treatment. BVS: bioresorbable vascular scaffold; DES: drug-eluting stent; MBF: myocardial blood flow; PET: positron emission tomography

post-dilatation was performed more frequently in comparison with DES. Although polymeric scaffold disruption due to overexpansion by post-dilation of BVS has been described, no scaffold fractures were observed in the present study^{20,21}. This is in line with recent evidence that post-dilatation in order to achieve scaffold optimisation does not result in (major) adverse cardiac events²². In contrast to some prior BVS studies^{7,9,11,12}, OCT analysis revealed comparable acute luminal areas post implantation between BVS and DES, which can be assigned to the higher rate of post-dilatation in the BVS group²³. Apart from one small side branch occlusion, no complications during BVS implantation were registered. However, despite the common occurrence of side branch occlusion during conventional stent implantation, the increased strut dimensions (150 μm vs. 80 μm for XIENCE) cannot be excluded as a contributing factor. Bail-out stenting for edge dissections was only required after DES implantation in two patients. Although this study was not powered to analyse BVS implantation characteristics and adverse cardiac events, these results confirm that BVS is safe and adequately implantable in type A or B1 coronary lesions if the prescribed implantation instructions are strictly respected.

COLD PRESSOR TEST

CPT is considered the gold standard to assess coronary artery vasomotor function in response to sympathetic stimulation²⁴⁻²⁶. An impaired response to this test is related to abnormal coronary endothelial and vascular smooth muscle cell function, and is associated with a risk of developing cardiovascular events^{24,27}. The purpose of including CPT MBF measurements in the present trial design was to evaluate the potential restoration of endothelial and vasomotor function upon final resorption of the scaffold. Compared with baseline, MBF of the treated vascular territory increased by $0.15 \pm 0.21 \text{ mL} \cdot \text{min}^{-1} \cdot \text{g}^{-1}$ during CPT, which is in line with previously reported values of patients with traditional CAD risk factors (i.e., hypertension, hypercholesterolaemia, or smoking) without flow-limiting CAD^{15,28}. At one-month follow-up, CPT MBF and CPT reserve were comparable between both treatment arms. This result was anticipated, as BVS retains its integrity for up to 12 months after implantation. The final results of the ongoing VANISH trial are awaited in order to assess the effects on CPT MBF of previously reported long-term vasomotor function restoration after BVS treatment.

HYPERAEMIC MYOCARDIAL PERFUSION AND CORONARY FLOW RESERVE

The primary goal of PCI is not to relieve anatomical blockage *per se* but to restore downstream myocardial perfusion. The present interim analysis has shown that hyperaemic MBF was comparable between both treatment arms, although CFR was significantly lower in the BVS treatment arm. CFR decreases if baseline perfusion is increased, as seen with a higher RPP. However, the level of significance increased when CFR was adjusted for the RPP of the baseline scan. Interestingly, the ratio of target CFR to remote CFR did not differ between both treatment arms, indicating a homogeneously attenuated global CFR. If anything, this would indicate a global effect of BVS on attenuating CFR and is therefore not explained by the previously observed smaller luminal area of BVS-treated coronary segments^{7,9,11,12}. In fact, as already alluded to, luminal dimensions were similar between BVS and DES as documented by OCT immediately after implantation. The hypothesised global effect of BVS on CFR in the present study is so far unexplained and requires further research. Although speculative, it could be hypothesised that in the early phase of BVS implantation global myocardial effects are exerted due to local vessel wall inflammation²⁹. The process of enhanced inflammation could theoretically be elicited by the degradation of the scaffold characterised by phagocytosis to assimilate small particles into lactate and finally pyruvate¹. It is likely that these inflammatory processes will dissipate over time as a porcine coronary artery model has demonstrated only minimal inflammation at two years after BVS implantation³⁰. Alternatively, the increased BVS strut dimensions result in low endothelial shear stress at the base of the struts, theoretically increasing neointimal growth and hampering normal coronary physiology, which possibly interferes with the vasoactive reactivity^{31,32}. Nevertheless, all these processes seem to appear locally and are unlikely to explain reduced global reactivity to hyperaemia satisfactorily. Although the treatment strategy was randomised, the possibility of *a priori* variation in baseline characteristics between treatment groups should be considered as a contributing factor.

Limitations

The specific device characteristics of BVS potentially increase the risk of periprocedural complications. Serruys et al previously demonstrated a slight increase of myocardial enzyme release after BVS implantation as compared to DES (5 vs. 2%, respectively)⁷. The present study design did not include periprocedural cardiac biomarker assessment, although periprocedural myocardial damage would be relevant with regard to the expected normalisation of myocardial perfusion and potential microvascular dysfunction.

Results of a globally attenuated CFR in the BVS treatment group suggest some degree of global microcirculatory impairment. However, without pre-interventional MBF and CFR data, these differences could be pre-existing, and no definite conclusions about an unequivocal relation between BVS and attenuated

global CFR should be drawn based on these data. The purpose of this study is to contribute to the understanding of the physiological processes during BVS resorption.

Conclusions

The present study shows that CFR is attenuated in BVS-treated patients, but neither BVS nor DES implantation leads to reduced myocardial perfusion. The comparable perfusion levels in both treatment arms, one month after implantation, do not offer an explanation for the recently reported lower cumulative rates of new or worsening angina in BVS-treated patients. Long-term results are awaited to determine whether vasomotor function will further improve after BVS resorption.

Impact on daily practice

Although CFR is attenuated in BVS-treated patients, implantation of a BVS seems safe without major consequences on short-term results with regard to myocardial perfusion.

Funding

This study was in part sponsored by Abbott Vascular and the Dutch Heart Foundation (Grant 2013T078).

Conflict of interest statement

The authors have no conflicts of interest to declare.

References

- Gogas BD, Farooq V, Onuma Y, Serruys PW. The ABSORB bioresorbable vascular scaffold: an evolution or revolution in interventional cardiology? *Hellenic J Cardiol.* 2012;53:301-9.
- Nakazawa G, Otsuka F, Nakano M, Vorpahl M, Yazdani SK, Ladich E, Kolodgie FD, Finn AV, Virmani R. The pathology of neo-atherosclerosis in human coronary implants bare-metal and drug-eluting stents. *J Am Coll Cardiol.* 2011;57:1314-22.
- Daemen J, Wenaweser P, Tsuchida K, Abrecht L, Vaina S, Morger C, Kukreja N, Jüni P, Sianos G, Hellige G, van Domburg RT, Hess OM, Boersma E, Meier B, Windecker S, Serruys PW. Early and late coronary stent thrombosis of sirolimus-eluting and paclitaxel-eluting stents in routine clinical practice: data from a large two-institutional cohort study. *Lancet.* 2007;369:667-78.
- Serruys PW, Garcia-Garcia HM, Onuma Y. From metallic cages to transient bioresorbable scaffolds: change in paradigm of coronary revascularization in the upcoming decade? *Eur Heart J.* 2012;33:16-25b.
- Serruys PW, Onuma Y, Dudek D, Smits PC, Koolen J, Chevalier B, de Bruyne B, Thuesen L, McClean D, van Geuns RJ, Windecker S, Whitbourn R, Meredith I, Dorange C, Veldhof S, Hebert KM, Sudhir K, Garcia-Garcia HM, Ormiston JA. Evaluation of the second generation of a bioresorbable everolimus-eluting vascular scaffold for the treatment of de novo coronary artery stenosis: 12-month clinical and imaging outcomes. *J Am Coll Cardiol.* 2011;58:1578-88.

6. Brugaletta S, Heo JH, Garcia-Garcia HM, Farooq V, van Geuns RJ, de Bruyne B, Dudek D, Smits PC, Koolen J, McClean D, Dorange C, Veldhof S, Rapoza R, Onuma Y, Bruining N, Ormiston JA, Serruys PW. Endothelial-dependent vasomotion in a coronary segment treated by ABSORB everolimus-eluting bioresorbable vascular scaffold system is related to plaque composition at the time of bioresorption of the polymer: indirect finding of vascular reparative therapy? *Eur Heart J*. 2012;33:1325-33.
7. Serruys PW, Chevalier B, Dudek D, Cequier A, Carrie D, Iniguez A, Dominici M, van der Schaaf RJ, Haude M, Wasungu L, Veldhof S, Peng L, Staehr P, Grundeken MJ, Ishibashi Y, Garcia-Garcia HM, Onuma Y. A bioresorbable everolimus-eluting scaffold versus a metallic everolimus-eluting stent for ischaemic heart disease caused by de-novo native coronary artery lesions (ABSORB II): an interim 1-year analysis of clinical and procedural secondary outcomes from a randomised controlled trial. *Lancet*. 2015;385:43-54.
8. Gomez-Lara J, Garcia-Garcia HM, Onuma Y, Garg S, Regar E, de Bruyne B, Windecker S, McClean D, Thuesen L, Dudek D, Koolen J, Whitbourn R, Smits PC, Chevalier B, Dorange C, Veldhof S, Morel MA, de Vries T, Ormiston JA, Serruys PW. A comparison of the conformability of everolimus-eluting bioresorbable vascular scaffolds to metal platform coronary stents. *JACC Cardiovasc Interv*. 2010;3:1190-8.
9. Serruys PW, Ormiston JA, Onuma Y, Regar E, Gonzalo N, Garcia-Garcia HM, Nieman K, Bruining N, Dorange C, Miquel-Hebert K, Veldhof S, Webster M, Thuesen L, Dudek D. A bioabsorbable everolimus-eluting coronary stent system (ABSORB): 2-year outcomes and results from multiple imaging methods. *Lancet*. 2009;373:897-910.
10. Ormiston JA, Serruys PW, Onuma Y, van Geuns RJ, de Bruyne B, Dudek D, Thuesen L, Smits PC, Chevalier B, McClean D, Koolen J, Windecker S, Whitbourn R, Meredith I, Dorange C, Veldhof S, Hebert KM, Rapoza R, Garcia-Garcia HM. First serial assessment at 6 months and 2 years of the second generation of absorb everolimus-eluting bioresorbable vascular scaffold: a multi-imaging modality study. *Circ Cardiovasc Interv*. 2012;5:620-32.
11. Brugaletta S, Radu MD, Garcia-Garcia HM, Heo JH, Farooq V, Girasis C, van Geuns RJ, Thuesen L, McClean D, Chevalier B, Windecker S, Koolen J, Rapoza R, Miquel-Hebert K, Ormiston J, Serruys PW. Circumferential evaluation of the neointima by optical coherence tomography after ABSORB bioresorbable vascular scaffold implantation: can the scaffold cap the plaque? *Atherosclerosis*. 2012;221:106-12.
12. Serruys PW, Onuma Y, Ormiston JA, de Bruyne B, Regar E, Dudek D, Thuesen L, Smits PC, Chevalier B, McClean D, Koolen J, Windecker S, Whitbourn R, Meredith I, Dorange C, Veldhof S, Miquel-Hebert K, Rapoza R, Garcia-Garcia HM. Evaluation of the second generation of a bioresorbable everolimus drug-eluting vascular scaffold for treatment of de novo coronary artery stenosis: six-month clinical and imaging outcomes. *Circulation*. 2010;122:2301-12.
13. Stuijzand W, Knaapen P. Impact of Vascular Reparative Therapy on Vasomotor Function and Myocardial Perfusion: a Randomized H2150 PET/CT Study (VANISH). [ClinicalTrials.gov Identifier: NCT01876589](https://clinicaltrials.gov/ct2/show/study/NCT01876589).
14. Danad I, Raijmakers PG, Appelman YE, Harms HJ, de Haan S, van den Oever ML, van Kuijk C, Allaart CP, Hoekstra OS, Lammertsma AA, Lubberink M, van Rossum AC, Knaapen P. Coronary risk factors and myocardial blood flow in patients evaluated for coronary artery disease: a quantitative [¹⁵O]H₂O PET/CT study. *Eur J Nucl Med Mol Imaging*. 2012;39:102-12.
15. Schindler TH, Nitzsche EU, Olschewski M, Brink I, Mix M, Prior J, Facta A, Inubushi M, Just H, Schelbert HR. PET-measured responses of MBF to cold pressor testing correlate with indices of coronary vasomotion on quantitative coronary angiography. *J Nucl Med*. 2004;45:419-28.
16. Lubberink M, Harms HJ, Halbmeijer R, de Haan S, Knaapen P, Lammertsma AA. Low-dose quantitative myocardial blood flow imaging using ¹⁵O-water and PET without attenuation correction. *J Nucl Med*. 2010;51:575-80.
17. Harms HJ, de Haan S, Knaapen P, Allaart CP, Lammertsma AA, Lubberink M. Parametric images of myocardial viability using a single ¹⁵O-H₂O PET/CT scan. *J Nucl Med*. 2011;52:745-9.
18. Austen WG, Edwards JE, Frye RL, Gensini GG, Gott VL, Griffith LS, McGoon DC, Murphy ML, Roe BB. A reporting system on patients evaluated for coronary artery disease. Report of the Ad Hoc Committee for Grading of Coronary Artery Disease, Council on Cardiovascular Surgery, American Heart Association. *Circulation*. 1975;51:5-40.
19. Ormiston JA, Serruys PW, Regar E, Dudek D, Thuesen L, Webster MW, Onuma Y, Garcia-Garcia HM, McGreevy R, Veldhof S. A bioabsorbable everolimus-eluting coronary stent system for patients with single de-novo coronary artery lesions (ABSORB): a prospective open-label trial. *Lancet*. 2008;371:899-907.
20. Onuma Y, Serruys PW, Ormiston JA, Regar E, Webster M, Thuesen L, Dudek D, Veldhof S, Rapoza R. Three-year results of clinical follow-up after a bioresorbable everolimus-eluting scaffold in patients with de novo coronary artery disease: the ABSORB trial. *EuroIntervention*. 2010;6:447-53.
21. Ormiston JA, De Vroey F, Serruys PW, Webster MW. Bioresorbable polymeric vascular scaffolds: a cautionary tale. *Circ Cardiovasc Interv*. 2011;4:535-8.
22. De Ribamar Costa J Jr, Abizaid A, Bartorelli AL, Whitbourn R, van Geuns RJ, Chevalier B, Perin M, Seth A, Botelho R, Serruys PW; ABSORB EXTEND Investigators. Impact of post-dilation on the acute and one-year clinical outcomes of a large cohort of patients treated solely with the Absorb Bioresorbable Vascular Scaffold. *EuroIntervention*. 2015;11:141-8.
23. Mattesini A, Pighi M, Konstantinidis N, Ghione M, Kilic D, Foin N, Dall'ara G, Secco GG, Valente S, Di Mario C. Optical coherence tomography in bioabsorbable stents: mechanism of vascular response and guidance of stent implantation. *Minerva Cardioangiol*. 2014;62:71-82.

24. Kiviniemi T. Assessment of coronary blood flow and the reactivity of the microcirculation non-invasively with transthoracic echocardiography. *Clin Physiol Funct Imaging*. 2008;28:145-55.
25. Rigo F, Murer B, Ossena G, Favaretto E. Transthoracic echocardiographic imaging of coronary arteries: tips, traps, and pitfalls. *Cardiovasc Ultrasound*. 2008;6:7.
26. Rigo F. Coronary flow reserve in stress-echo lab. From pathophysiologic toy to diagnostic tool. *Cardiovasc Ultrasound*. 2005;3:8.
27. Schindler TH, Nitzsche EU, Schelbert HR, Olschewski M, Sayre J, Mix M, Brink I, Zhang XL, Kreissl M, Magosaki N, Just H, Solzbach U. Positron emission tomography-measured abnormal responses of myocardial blood flow to sympathetic stimulation are associated with the risk of developing cardiovascular events. *J Am Coll Cardiol*. 2005;45:1505-12.
28. Siegrist PT, Gaemperli O, Koepfli P, Schepis T, Namdar M, Valenta I, Aiello F, Fleischmann S, Alkadhi H, Kaufmann PA. Repeatability of cold pressor test-induced flow increase assessed with H(2)(15)O and PET. *J Nucl Med*. 2006;47:1420-6.
29. Jiang WW, Su SH, Eberhart RC, Tang L. Phagocyte responses to degradable polymers. *J Biomed Mater Res A*. 2007;82:492-7.
30. Onuma Y, Serruys PW, Perkins LE, Okamura T, Gonzalo N, Garcia-Garcia HM, Regar E, Kamberi M, Powers JC, Rapoza R, van Beusekom H, van der Giessen W, Virmani R. Intracoronary optical coherence tomography and histology at 1 month and 2, 3, and 4 years after implantation of everolimus-eluting bioresorbable vascular scaffolds in a porcine coronary artery model: an attempt to decipher the human optical coherence tomography images in the ABSORB trial. *Circulation*. 2010;122:2288-300.
31. O'Brien CC, Kolachalama VB, Barber TJ, Simmons A, Edelman ER. Impact of flow pulsatility on arterial drug distribution in stent-based therapy. *J Control Release*. 2013;168:115-24.
32. Bourantas CV, Papafaklis MI, Kotsia A, Farooq V, Muramatsu T, Gomez-Lara J, Zhang YJ, Iqbal J, Kalatzis FG, Naka KK, Fotiadis DI, Dorange C, Wang J, Rapoza R, Garcia-Garcia HM, Onuma Y, Michalis LK, Serruys PW. Effect of the endothelial shear stress patterns on neointimal proliferation following drug-eluting bioresorbable vascular scaffold implantation: an optical coherence tomography study. *JACC Cardiovasc Interv*. 2014;7:315-24.